Second International Conference on CFD in the Minerals and Process Industries
CSIRO, Melbourne, Australia
6-8 December 1999

METHODS, CAPABILITIES AND APPLICATION OF THE COMBUSTION SIMULATION PROGRAM FIRE3D/RF

Ralf VONDERBANK[1] and Terry JOHNSON[2]

[1]Fire3D Software Development, 51588 Nuembrecht, GERMANY
[2]HRL Herman Research Pty Ltd, Mulgrave, Victoria 3170, AUSTRALIA

ABSTRACT

Reliable and economical CFD methods and programs become more important for the industry, in particular because of the availability of well-proved physico-mathematical models and advanced numeric solution techniques. This contribution is focused on the numerical solution techniques, the physico-mathematical methods, the capabilities and application of the Fire3D/R4 program.

For the first time the advanced direct pressure calculation scheme ADDIP (instead of pressure and velocity correction methods) and the implemented numerical procedure to solve the set of partial differential transport equations of momentum, enthalpy, turbulence and species (suspending fluid) is presented.

The employed combustion model is based on a two step reaction model for gases and coal particles. A further developed EDC three component model is used to model the simultaneous combustion of CO, BG (burning gas, defined by the number of H/C atoms) and CHO (a carbon-hydrogen-oxygen molecule with a composition based on the ultimate analysis of the coal and which is released during pryolytic decomposition as the volatile matter of coal). The incorporated model of heterogeneous reactions on the surface of the coal particles considers carbon dioxide in addition to oxygen as concurrent reactants. In all reactions with gases and coal, the C atoms are converted in a first step to carbon monoxide, which forms carbon dioxide in a second step (if kinetic conditions and turbulent mixing allow this reaction). The H atoms of BGT and CHO directly react during the first step to form water vapor.

The combustion process inside the furnace of the brown coal fired steam generator Yallourn W Stage 1 (nominal thermal capacity of 1060 MJ/s) was numerically studied and compared with experimental data. Good agreement was found.

NOMENCLATURE

cp	thermal capacity	κ	absorption coef
h	enthalpy	κ_t	von Karman const.
I	radiation intensity	μ_t	turb. viscosity
k_t	turb. Energy	ν	kinematic viscosity
T	temperature	ξ	concentration
x	length	ρ	density
α	species	τ	time, shear stress
$\delta_{i\varphi}$	Kronecker delta	ϕ	phys. property
ε	emissivity	ω	relaxation factor
ε_τ	eddy dissipation	C,E,PP	model const.

INTRODUCTION

The actual history of the development of Fire3D began in the fall of the year 1994. At that time the decision was taken to develop a simulation program. It should be optimized for flows with combustion and radiation. At first there were definitions with regard to grid generation, method of grid discretization and solution algorithms. In spring 1998, the first release suitable for the industry was available.

For the rest of the year the work was focussed on the development of an advanced, modern algorithm for the calculation of pressure fields.

The first trials, based on a Poisson equation, had little success. The Poisson equation was derived from the three momentum equations. There were difficulties when incompressibility of the flow field, i.e. constant density, was assumed. The mathematical problem becomes overdefined. Finally, it becomes necessary to introduce formulations for a velocity correction in order to fulfil the equations of continuity and momentum. These formulations would replace the method of pressure correction.

Eventually the advanced direct pressure calculation scheme ADDIP was discovered by trying and guessing. The testing of the ADDIP scheme was very successful and subsequently it got a decisive role within the program code of Fire3D.

MODEL DESCRIPTION

The orthogonal grid

A natural choice of geometries of industrial firing systems such as brown coal fired furnaces are orthogonal, rectangular grids, because of the ease to generate them, especially for 3D configurations. An additional advantage is that no curvature terms appear in the transport equations. For such geometries the surfaces of the body, i.e. the membrane walls, coincide with the faces of the finite volume elements and subsequently the coordinate system is body-fitted.

The grid is non-staggered. All dependent variable for the various transport equations and all physical quantities are defined in the centre of gravity of the finite volume elements. The inlet conditions are defined in the center of the corresponding surface element.

The inlets and outlets

Usually, there are three different types of inlets and outlets necessary to describe existing openings in membrane walls.

Typical these are the inlets (1) of the burner openings for the pulverized coal with the conveying gas or primary air, beside hot secondary, tertiary, over fire air or recirculated tempering gas. Here, all inlet conditions like velocity components, turbulence (eddy dissipation, kinetic energy), temperature, species concentrations, fuel load and enthalpy have to be defined.

At the typical outlet (2), like the end of the furnace where the flue gases enter the convection pass, none of the above mentioned physical conditions have to be defined in advance.

The last type (3) of opening is the negative inlet, where only the velocity components have to be defined. The other physical conditions are solely a result of the iterative solving procedure of all coupled transport equations.

Typical for this kind of negative inlets are the opening of the dryer shafts where hot flue gas is drawn off the furnace towards each ventilating beater wheel mill in service.

Because of the importance of type two there are three more subdivisions of this kind of inlets regarding the gas compositions. Firstly, by default, the program assumes that hot air, at a given temperature, flows into the furnace. Secondly, it is impossible to assign to any inlet element a given gas composition. Thirdly, another given gas composition, carrying pulverized fuel, is assigned to inlets.

The composition of the pulverized fuel has to be given by the appropriate values of the coal analysis. The mean diameter of the particulates represents the spectrum of the particle classes of the coal dust conveyed into the furnace.

The concept of discretization

A generalized transport equation consists of terms describing convection, diffusion/conduction and sources or sinks. Some suggestions of Patanker (1984) were followed. An upwind-difference scheme is applied for the discretization of the convection terms in order to get a better, realistic prescription of convected properties at the interfaces of the finite volume elements.

Diffusion/conduction terms are discretized by a central-difference scheme. A backward-difference in time is used for the transient term.

The discretized, generalized transport equation (1) is presented here:

$$\left[\frac{\varrho(N)}{\Delta\tau}\cdot VOL(N)+FE(N)+FW(N)+FN(N)+FS(N)+FT(N)+FB(N)\right]\cdot\Phi^{n+1}(N)= FE(N)\cdot\Phi^{n}(NE)+FW(N)\cdot\Phi^{n}(NW)+FN(N)\cdot\Phi^{n}(NN)+FS(N)\cdot\Phi^{n}(NS)+FT(N)\cdot\Phi^{n}(NT)+FB(N)\cdot\Phi^{n}(NB)+\frac{\varrho(N)}{\Delta\tau}\cdot VOL(N)\,\Phi^{n}(N)+SST(N) \qquad (1)$$

Although it is frequently reported that tridiagonal matrix algorithms, when extended for multiple dimensions, show high performance, explicit methods are to be preferred. It is our experience that explicit methods are not more complicated and that they do not require more computer time and storage. In Fire3D the Gauß-Seidel method is realised. It is possibly the simplest of all available iterative procedures. Eq.(1) can be rearranged:

$$\Phi^{n+1}(N) = \ldots\ldots \qquad (2)$$

The relaxation

Because of the strongly nonlinear character of the transport equations underrelaxation is used to increase the numerical stability and to avoid divergence.

The absolute value of the relaxation factor is smaller than unity. The larger the relaxation factor the faster the numerical solution proceeds. Subsequently it is of advantage if there is a way to adapt the value of the relaxation factors during the running iterative process.

$$0.2 \le \omega_{\alpha} \le 0.01 \qquad (3)$$

The relaxation factors ω of the transport equations α can be manipulated and changed during the program run in order to maximized the performance of the calculation. At the beginning of a calculation the inertia of mass or ignition of fuel are significant obstacles which prevent the choice of high relaxation factors. After a certain computing time or number of iterations the relaxation factors can be increased.

Table 1: Transport equations

ϕ	
u, v, w	velocity components
h	enthalpy
k_t	kinetic energy of turbulence
ε_t	eddy dissipation of turbulence
O_2	content of oxygen
CO	content of carbon monoxide
H_2O	content of moisture
CO_2	content of carbon dioxide
$Coal$	content of coal
Ash	content of mineral matter of coal
$Char$	content of char of coal
$CHONS$	content of volatile matter of coal
BG	content of burning gas [$C\alpha H\beta$]
$SFX\pm$	radiative flux pos/neg x direction
$SFY\pm$	radiative flux pos/neg y direction
$SFZ\pm$	radiative flux pos/neg z direction

The transport equations

There are a total set of 21 transport equations, listed in Table 1.

The three velocity components u, v and w are calculated by solving the three Navier-Stokes, momentum equations for a compressible and viscous fluid. The density ρ of the suspension depends on the consistency of the fluid (content and type of gas and solid species), pressure and temperature and is calculated in a separate subroutine. The concentration of nitrogen is not determined by a transport equation. The fact is applied that the sum of all species concentrations is equal unity. Subsequently the content of nitrogen can be calculated by the algebraic relation:

$$\xi_{N} = 1 - \sum \xi_{\alpha,gas,solid} \qquad (4)$$

The transport equations are solved by a separate numerical procedure which is different from the Gauß-Seidel algorithm in conjunction with Eq.1. This and the other models are described in more detail below.

The residuals

The size of the absolute values of the residuals are indicators of the progress of the numeric iterative calculation procedure. Hence, the residuals are subject of continuous supervision. There is a key implemented which allows to choose how often the program has to write the residuals into an appropriate file: after 1, 10 or 100 iterations.

The generalized form of the calculation method of the residuals is given in Eqs. 5 which is derived from Eq. 1, in which AP(N) is the multiplier of Φ^{n+1}on the left side of Eq.1. The residuals for radiation flux and pressure will be presented in the corresponding sections.

$$RST = \varrho(N)\cdot VOL(N)/\tau \qquad (5.1)$$

$$RS_{\alpha} = RST\cdot\Phi_{\alpha}^{n}(N) + SST_{\alpha} \qquad (5.2)$$

$$F_{\alpha} = FE(N)\cdot\Phi_{\alpha}^{n}(NE) + FW(N)\cdot\Phi_{\alpha}^{n}(NW) + FN(N)\cdot\Phi_{\alpha}^{n}(NN) + FS(N)\cdot\Phi_{\alpha}^{n}(NS) + FT(N)\cdot\Phi_{\alpha}^{n}(NT) + FB(N)\cdot\Phi_{\alpha}^{n}(NB) \qquad (5.3)$$

$$RES_{\alpha} = F_{\alpha} - AP(N)\cdot\Phi_{\alpha}^{n}(N) + RS_{\alpha} \qquad (5.4)$$

The temperature iteration

The emthalpy and heat capacity depend on temperature and are expressed by polynomial series of 5th order. The temperature is iteratively evaluated by Newton's approximation:

$$T_{m+1} = T_{m} - \frac{h(T_m)}{cp(T_m)} \qquad (6)$$

After each iterative loop over the equations of transport one step of the Newton approximation is performed. The polynomials of enthalpy and heat capacity are taken from the FDBR manual.

The density

Calculation of density is performed with consideration of temperature and fluid composition. The mass specific volumes of the gas and solid phases (denoted SV) are calculated and used to determine the density:

$$SV_{Gas} = \sum \frac{\Phi_{Gas,\alpha}}{\varrho_{0,Gas,\alpha}} \qquad (7.1)$$

$$SV_{Solid} = \sum \frac{\Phi_{Solid,\alpha}}{\varrho_{0,Solid,\alpha}} \qquad (7.2)$$

$$\varrho_{Suspension} = \frac{1}{SV_{Gas}\cdot\Pi_{T}\cdot\Pi_{P} + SV_{Solid}} \qquad (7.3)$$

The turbulence model

A standard two equation model is applied in which the tensor of the velocity correlations is given by:

$$-\overline{u'_i u'_j} = C_{\mu}\frac{k_t^2}{\varepsilon_t}\left[\left(\frac{\partial\overline{u_i}}{\partial x_j}+\frac{\partial\overline{u_j}}{\partial x_i}\right) - \frac{2}{3}\frac{\partial\overline{u_k}}{\partial x_k}\delta_{ij}\right] - \frac{2}{3}k_t\delta_{ij} \qquad (8)$$

For the derivation of the transport equation of the kinetic turbulent energy and the eddy dissipation, see for instance Vonderbank(1995), Wirtz (1989) or Zinser (1985).

In general, the proposals of Launder, Spalding, Pope, Lumley, Jones and Janicka were followed.

$$\bar{\varrho}\left(\frac{\partial k_t}{\partial\tau} + \overline{u_k}\frac{\partial k_t}{\partial x_k}\right) = \bar{\varrho}\frac{\partial}{\partial x_k}\left[\left(\frac{\upsilon_t}{\sigma_k}+\upsilon\right)\frac{\partial k_t}{\partial x_k}\right] - \bar{\varrho}\,\overline{u'_i u'_k}\frac{\partial\overline{u_i}}{\partial x_k} - \bar{\varrho}\,\varepsilon_t \qquad (9.1)$$

$$\bar{\varrho}\left(\frac{\partial\varepsilon_t}{\partial\tau} + \overline{u_k}\frac{\partial\varepsilon_t}{\partial x_k}\right) = \bar{\varrho}\frac{\partial}{\partial x_k}\left[\left(\frac{\upsilon_t}{\sigma_\varepsilon}+\upsilon\right)\frac{\partial\varepsilon_t}{\partial x_k}\right] - C_1\,\bar{\varrho}\,\frac{\varepsilon_t}{k_t}\,\overline{u'_i u'_k}\frac{\partial\overline{u_i}}{\partial x_k} - C_2\,\bar{\varrho}\,\frac{\varepsilon_t^2}{k_t} \qquad (9.2)$$

The dynamic, turbulent viscosity of the fluid is given by:

$$\mu_t = C_{\mu}\,\bar{\varrho}\,\frac{k_t^2}{\varepsilon_t} \qquad (9.3)$$

The modelling of the eddy viscosity in Eq. 9.3 is valid for a clean flow and has to be corrected for a particle-laden fluid with Abramovich's model (see Melville, Bray 1979), because the loading of particles leads to an increase in the turbulent energy dissipation:

$$\frac{\mu_t}{\mu_{t,0}} = \left(1+\frac{\sum\xi_{\alpha,solid}}{\sum\xi_{\alpha,gas}}\right)^{-1} \qquad (9.4)$$

The combustion model

For the detailed description of the combustion model refer to Vonderbank (1995) pp. 125-134. An overview of the physico-chemical model and the numerical procedure is presented in the following figure and text.

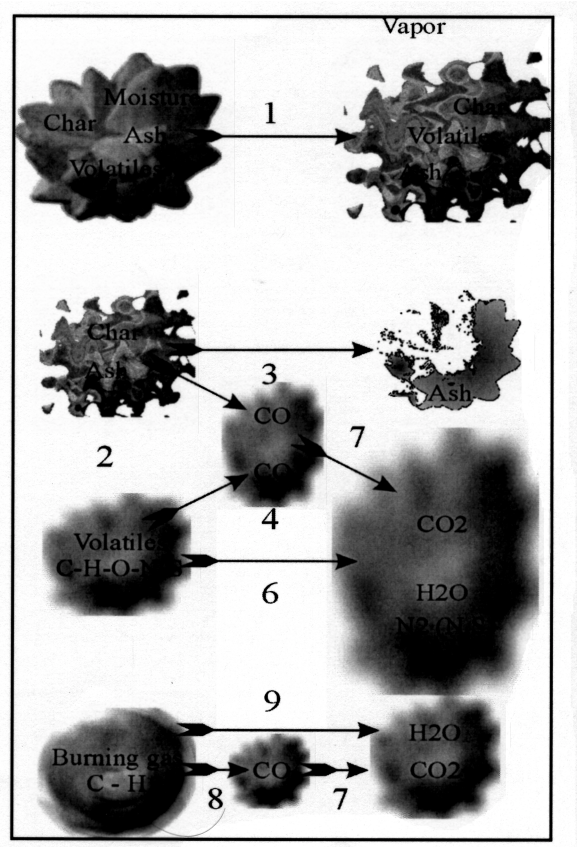

Figure 1: Schematic diagram of the combustion process.

In reality the vaporization of the residue moisture in the coal particles begins after the moment when they have entered the furnace through the burner slots. The residue moisture of brown coal after the combined milling and drying process within the beater wheel mills varies but is usually around 20%. This moisture has to be released during the very first moment after the particles enter the furnace due to the immense rate of heat transferred to the particles. To cover this process mathematically there are two possibilities. Firstly, an energy balance of the particle phase has to be considered. This has the disadvantage of additional need for computing power. And secondly, a rather trivial assumption can be followed. It may be assumed that the entire moisture is vapourized during the drying process.

During the early stages of the up-heating the thermal destruction (pyrolysis) of the particles occurs. Because of the significance of the volatile matters for the ignition and therefore for the entire combustion process it is most important to model the devolatilization accurately. A first order ordinary differential equations is used to describe the release of volatiles. The kinetic coefficients were taken from Duong (1985).

The atomic composition and the corresponding heating value of the volatiles are calculated from an atom and energy balance.

Combustion of the volatiles can take place if mixing with an oxygen containing gas (air or flue gas) occurs. Mixing happens primarily by convection in macroscopic length scales and secondary by viscous/turbulence phenomena or tertiary by diffusion effects. Turbulence is working in microscopic length scales and is effectively enhancing diffusion and viscosity. Only if mixing is perfect a chemical Arrhenius differential equation may be used for the prediction of the combustion rates.

An extended Eddy Dissipation Concept (EDC) is applied here. The original model was developed by Magnussen and Hjertager (1976). In the extended EDC the fast chemistry approach is followed. In both cases, volatiles and burning gas, the hydrogen atoms form vapor. The carbon atoms convert to carbon monoxide if the mixing conditions are fulfilled.

In a second step the carbon monoxide reacts to carbon dioxide by oxidation. The oxidation of carbon monoxide is relatively slowly, subsequently the kinetic rate of oxidation has to be considered. Accordingly, the mixing condition of the EDC has to be satisfied and the maximally possible rate is evaluated by a kinetic Arrhenius approach. The kinetic reaction rates for carbon monoxide were taken from Howard, Williams and Fine (1973).

The oxidation of char is controlled by diffusion in the regime of high temperatures and by the heterogeneous kinetic reaction on the surface of the particles in the regime of low temperatures. The well-known model of Field, Gill, Morgan and Hawskley (1967) is applied although more detailed descriptions are available. But because of uncertainties, modelling of the char combustion process has been highly dependent on laboratory rate data for the specific coal and depends also on the test conditions.

The kinetic factors for the competing Boudouard reaction with carbon dioxide were taken from the works of Schneyder and Mitchell and Madsen (1986).

The set of ordinary differential equations for the combustion model is solved by an explicit forward-in-time difference scheme (see Figure 2).

The radiation transport and transfer

a) Radiation transport model

The model of radiation transport was developed for the economic use of computing power. It represents a combination of a three dimensional flux method and the discrete transfer method (compare Kühlert, 1998). The simplified radiation transport equation is:

$$\frac{dI(s)}{ds} = -\kappa(s)\cdot I(s) + \kappa(s)\cdot I_b(s) \qquad (10.1)$$

Integration over ds leads to the following expressions:

$$I_{s+1}^{n+1} = I_s^n \cdot \exp(-\kappa\cdot\Delta x) + I_b \cdot (1-\exp(-\kappa\cdot\Delta x)) \qquad (10.2)$$

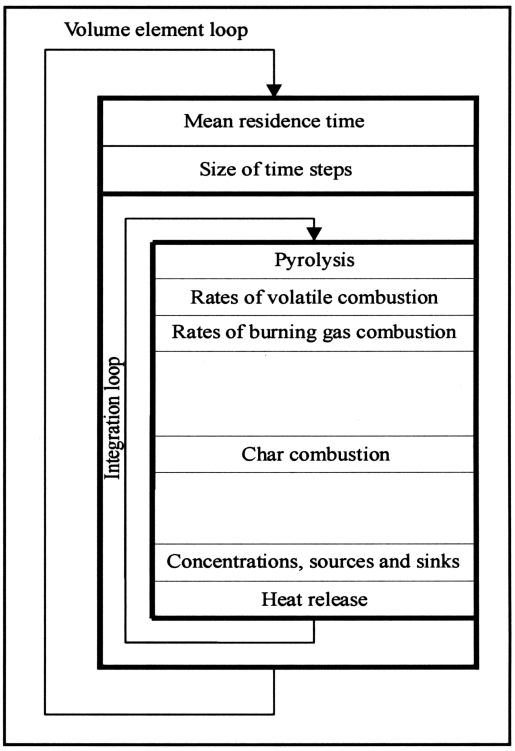

Figure 2: Schematic diagram of the numerical integration process in the combustion model.

When Eq. 10.2 is integrated over the surface area, which is normal to the coordinate s, an equation for the radiation energy is formulated. This equation is used to compute the energy transport for all six flux directions.

The emitted radiation I_b is distributed to all six discrete directions of the Cartesian coordinate system proportionally to the area size of the faces of the finite volume elements.

This model is accurate for radiating gases and suspensions with high optical thickness like in furnaces and of most flames of technical firing systems. The disadvantage is that this model has the need to store two time levels but has the important advantage that the calculation procedure (10.2) of three radiation fluxes saves computing power.

b) Emissivity

A grey gas – emissivity model is applied. The gas species under consideration are H_20, CO_2, N_2, O_2 and CO. Other species have low concentrations and their effect on radiation properties is usually neglectable. Symmetric molecules like N_2 and O_2 do not emit photons even at elevated temperatures. Carbon monoxide has some effect on the emissivity of a radiating gas. Here it is neglected. Gas radiation is emitted in spectral lines which often emerge as spectral bands because of their number broadening and overlapping. The spectral bands of H_2O and CO_2 lie in the infra-red region of light. The emissivity of a gas depends on the gas volume which is emitting the radiation: The longer the length of the beam, the higher the emissivity. The law of Beer-Lambert gives:

$$\varepsilon_{radiation} = 1 - \exp(-\kappa \cdot L) \qquad (11.1)$$

The bands of radiative emission for H_2O and CO_2, overlap. Subsequently both gases absorb radiation from each other. It follows when both gas components are present the total emissivity is smaller than the sum of both emissivities. The calculated sum of both emissivities has to be corrected by a correction term or this effect has to be considered by the calculation procedure (and the underlying experimental data).

Hence, a set of approximations for the grey gas emissivity of gas mixtures of H_2O and CO_2 are applied. These approximations were selected from Farag and Allam (1976-1982) and Hottel (1985). The selected set of approximations can be found in Vonderbank (1996, 1997). It comprises approximations for pure H2O and CO2 and three gas mixtures with the partial pressure ratios: ½, 1 and 2, Linear inter- and extrapolations are performed between the five different pressure ratios.

Since there is a certain particle load in the gases, resulting from the unburnable mineral matter of the coal (usually ash) and the pulverized coal particle itself, a suggestion of Richter, Michelfelder and Vortmeyer (1994) is used (see for details Vonderbank, 1996, 1997). Eventually, the total emissivity of both grey gas and particles is given by the relation:

$$\varepsilon_{rad.tot.} = \varepsilon_{part.} + \varepsilon_{gas} - \varepsilon_{part.} \cdot \varepsilon_{gas} \qquad (11.2)$$

It should be noted that because of the different side lengths of the finite volume elements anisotropy is considered by the use of three side length dependent total emissivities and three absorption coefficients.

The boundary conditions

a) Turbulence

The values of k_t and ε_t next to the wall are given by the following expression:

$$\varepsilon_{t,W} = C_\mu^{3/4} \frac{k_{t,W}^{3/2}}{\kappa_t \, \overline{\Delta x_P}} \quad (12.1) \qquad k_{t,W} = C_\mu^{-1/2} \frac{\tau_W}{\varrho} \quad (12.2)$$

b) Wall friction

The universal "Logarithmic Distribution Law" is applied to calculate the wall friction stress (compare for details Zinser, 1985):

$$\tau_W = \frac{\kappa_t \, C_\mu^{1/4} \, \varrho \, k_{t,W}^{1/2} \, |u|}{\ln \left(E_t \, C_\mu^{1/4} \, k_{t,W}^{1/2} \, \overline{\Delta x_P} \, \upsilon^{-1} \right)} \qquad (12.3)$$

c) Conductive heat transfer

The heat transfer model is taken from Bruneaux, Akselvoll, Poinsot and Ferzinger (1996) which is based on the von Karman – Reynolds analogy and leads to:

$$q_W = \frac{\kappa_t \, C_P \, \varrho \, (\tau_w/\varrho)^{1/2} \cdot (T_W - T)}{Pr_t \left(\ln \left(E_t \, C_\mu^{1/4} \, k_t^{1/2} \, \overline{\Delta x} \, \upsilon^{-1} \right) + PP_t \right)} \qquad (12.4)$$

d) Radiative heat transfer

It is assumed that both absoptivity and emissivity of the wall are equal. The emitted plus reflected radiation which is denoted as J is proportionally split into the other possible flux directions according to the sizes of the faces of the finite volume element.

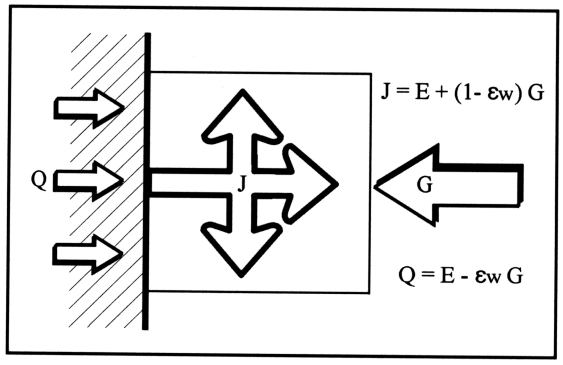

Figure 3: Schematic of the boundary conditions of radiative heat transfer

SIMULATION RESULTS

As a test case the combustion within the furnace of the steam generator of the unit Yallourn W Stage 1 was numerically simulated with Fire3D. This is a unit with an output of 350 MWe. It is fired with brown coal from the LaTrobe Valley.

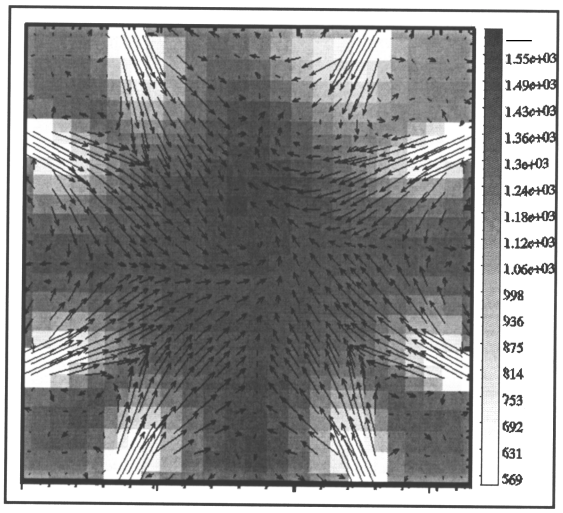

Figure 4a: Temperature (^{o}K) distribution inside the combustion chamber at 1st main burner level. The tangential arrangement of the burners is shown.

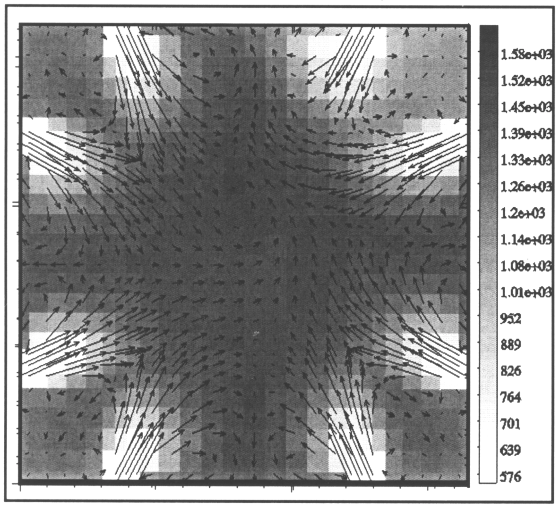

Figure 4b: Temperature (^{o}K) distribution inside the combustion chamber at 1st main burner level. The upper right mill is out off operation.

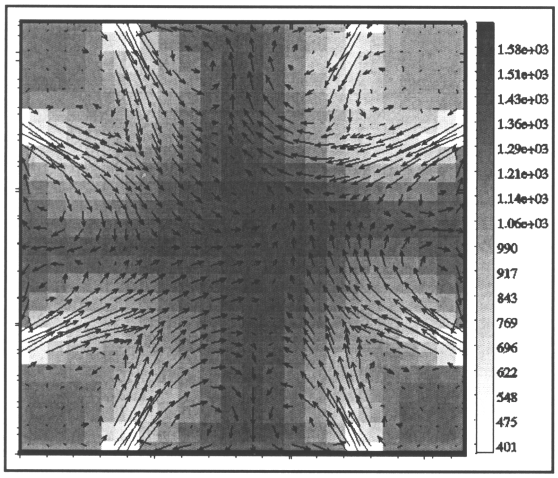

Figure 4c: Temperature (^{o}K) distribution inside the combustion chamber at vapor burner level. Cooling air enters through the air tubes (cruciform arrangement) of the burners of the mill out-off operation.

The overall arrangement of Figure 5 shows the positions of the ash hopper, the 1st and 2nd main burner levels, the vapor burners above, the flue gas resuction heads and the begin of the convection banks at the upper end of the furnace. The furnace from the hopper to its end is discretized by 28X28 finite volume elements (FVE) in the horizontal plane and 78 planes of FVEs over the height, which is a total of 58,016 FVEs.

The computing performance

The required memory is 58MB for this configuration. The simulation was performed on a PentiumPro-based PC with 200 MHz on a single processor. The elapsed computing time was 14 days while 76,630 iterations were performed which represents about 5,500 iterations per day.

Due to the fact that the program is written in C and Fortran it is possible to run it on almost every platform because of the availability of the appropriate compilers.

In Table 2 the sums of the residua at the end of the simulations are summarized. Their tiny size shows convergence.

Continuity	1.0731E-03	SFX+	1.6865E-03
u	1.0776E-02	SFX-	1.6865E-03
v	8.6679E-03	SFY+	1.6836E-03
w	1.2128E-02	SFY-	1.6836E-03
Enthalpy	0.7417E-01	SFZ+	1.7235E-03
ε_t	9.3850E-02	SFZ-	1.7235E-03
k_t	4.4619E-02	O2	5.5051E-05
Ash	3.3522E-07	CO2	8.0284E-05
Coal	2.2743E-06	H20	9.6206E-05
Char	2.4742E-06	CO	6.9650E-06
CHONS	2.2200E-06	BG	2.00093-122

Table 2: Residuals

All variables in Fire3D are defined using the DOUBLE PRECISION declaration which provides a considerable accuracy.

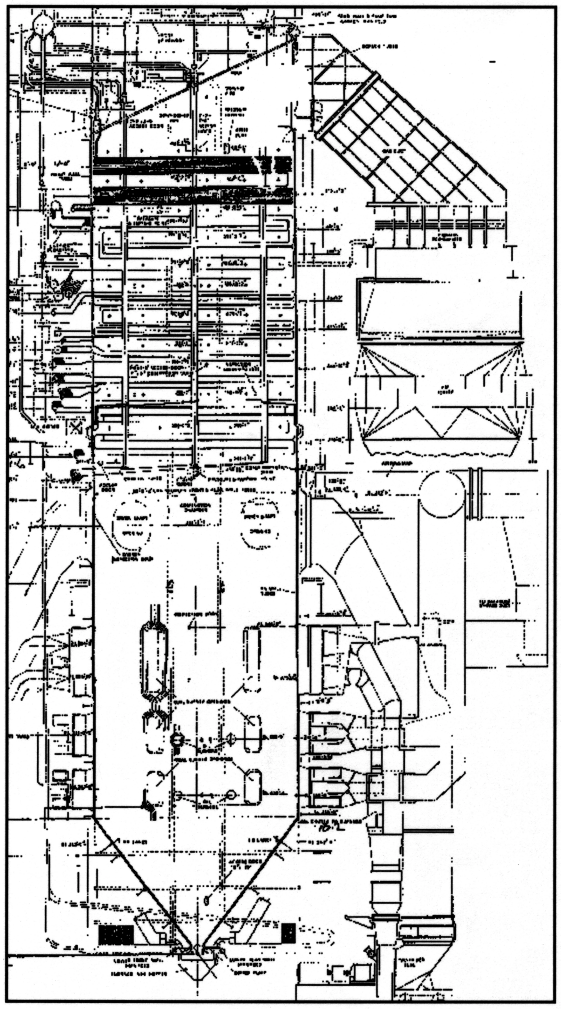

Figure 5: Overall furnace arrangement

Comparison with measurements

The results of the simulation are compared with measurement values of temperature from the end of the furnace and a distribution of incidental, radiation flux over the height of the furnace. The results are presented in Figure 6 and 7:

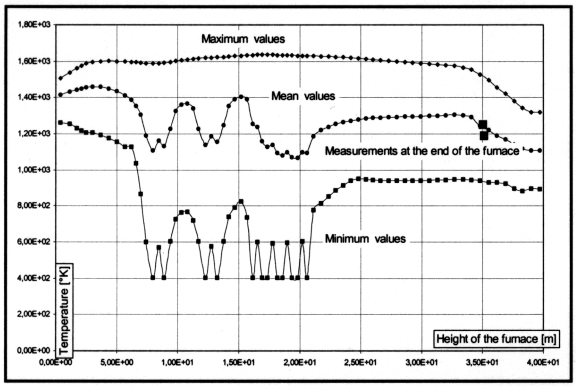

Figure 6: Temperature profiles

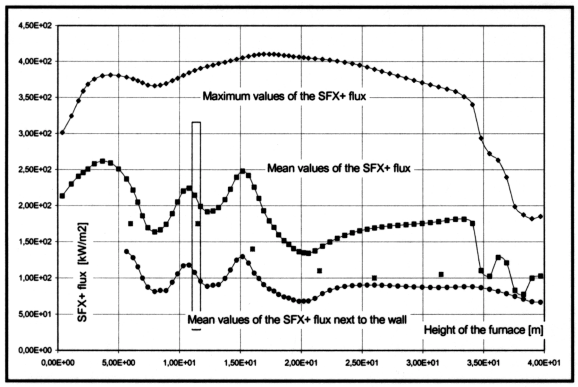

Figure 7: Flux profiles

Figure 6 shows that the measured temperatures at the end of the furnace are in good agreement with the calculated mean values of the combustion simulation. Consequently, it can be concluded that the total heat transfer process is properly modelled, i.e. the integral sum of radiative and convective transfer.

Although it is quite difficult to verify a heat transfer model with experimental data from a furnace of a steam generator, it is done here, as can be depicted from Figure 7.

Six measured values of radiation flux are compared with simulated mean values. In the upper furnace a good agreement between the mean values of the cell lines next to the wall of the simulated radiative flux with the measured data is shown. In the region of the burners, the measured values lie between the mean values of the cell lines next to the wall and the planar mean value of the entire FVE plane. It should be noted that the local differences of radiative flux can become relatively large along the furnace wall due to the immense local heat release rates.

FUTURE DEVELOPMENTS

The next step in developing Fire3D will be the implementation of local grid refinement techniques.

REFERENCES

BRUNEAUX, G., AKSELVOLL, K., POINSOT, T., FERZINGER, J.H., *Flame-wall interaction simulation in a turbulent channel flow,* Combustion and Flame 107: 27-44 (1996)

DUONG, T.H., *Mathematical modelling of pulverized Victorian brown coal combustion and heat transfer in a plug flow reactor,* Third Australian Conference on Heat Transfer, University of Melbourne, (1985)

FARAG, I.H., *Radiative heat transmission from non-luminous gases,* Doctoral thesis, MIT, (1976)

FARAG, I.H., Allam T.A., *Gray-gas approximation of carbon dioxide standard emissivity,* Journal of Heat Transfer, May 1981, Vol. 103

FARAG, I.H., Allam T.A., *A mixed grey-gas model to calculate water vapor standard emissivity,* ASME Publication 81-HT-63, (1981)

FARAG, I.H., ALLAM, T.A., *Carbon dioxide standard emissivity by mixed grey-gases model,* Chem. Eng. Commun., Vol.14, (1982)

FIELD, M.A., GILL, D.W., MORGAN, B.B., HAWKSLEY, P.G.W., *Combustion of pulverized coal,* BCURA, (1967)

HOTTEL, H.C., *Radiation from carbon dioxide, water vapor and soot,* American Flame Committee, MIT, (1985)

HOWARD, J.B., WILLIAMS, G.C., FINE, D.H., *Kinetics of carbon monoxide oxidation in postflame gases,* 14th Symp. (Int.) on Combustion, (1973)

KÜHLERT, K., *Modellbildung und Berechnung der Wärmestrahlung in Gas- und Kohlenstaubfeuerungen* Dissertation, Aachen, Shaker, (1998)

MAGNUSSEN, B.F., HJERTAGER, B.H., *On the mathematical modelling of turbulent combustion with special emphasis on soot formation and combustion,* 16th Symp. (Int.) on Combustion, (1976)

MITCHELL, R.E., MADSEN, O.H., *Experimentally determined overall burning rates of pulverized coal chars in specified O2 and CO2 environments,* 21st Symp. (Int.) on Combustion, (1986)

PANTANKAR, S.V., *Numerical heat transfer and fluid flow,* Hemisphere Pub., McGraw-Hill, (1980)

RICHTER, W., MICHELFELDER, S., VORTMEYER, D., *Wärmestrahlung in Brennräumen,* VDI-Wärmeatlas, 7.Auflage, (1994)

VONDEREBANK, R.S., *Untersuchung der Nox-, CO- und SO2-Schadstoffemissionen braunkohlegefeuerter Großkraftwerke,* Fortschr.-Ber. VDI Reihe 6 Nr.321, VDI-Verlag (1995), Dusseldorf

VONDERBANK, R.S., *CFD-Simulation der Kohleverbrennung in Großfeuerungsanlagen,* Teil 2, Brennstoff-Wärme-Kraft BWK Bd.48 (1996) Nr.10

VONDERBANK, R.S., *CFD simulations on a coal-coal reburning test facility,* International Journal of Energy Research, Vol.21, 985-1010 (1997)